CHIN. PHYS. LETT. Vol. 34, No. 5 (2017) 054701

Effect of Cellular Instability on the Initiation of Cylindrical Detonations *

Wen-Hu Han(韩文虎)[1], Jin Huang(黄金)[2**], Ning Du(杜宁)[1], Zai-Gang Liu(刘再刚)[1], Wen-Jun Kong(孔文俊)[1], Cheng Wang(王成)[3]

[1]*Key Laboratory of Light-Duty Gas-Turbine, Institute of Engineering Thermophysics, Chinese Academy of Sciences, Beijing 100190*
[2]*Beijing Priority Laboratory of Earthquake Engineering and Structural Retrofit, Beijing University of Technology, Beijing 100124*
[3]*Key Laboratory of Explosion Science and Technology, Beijing Institute of Technology, Beijing 100081*

(Received 18 November 2016)

The direct initiation of detonations in one-dimensional (1D) and two-dimensional (2D) cylindrical geometries is investigated through numerical simulations. In comparison of 1D and 2D simulations, it is found that cellular instability has a negative effect on the 2D initiation and makes it more difficult to initiate a sustaining 2D cylindrical detonation. This effect associates closely with the activation energy. For the lower activation energy, the 2D initiation of cylindrical detonations can be achieved through a subcritical initiation way. With increasing the activation energy, the 2D cylindrical detonation has increased difficulty in its initiation due to the presence of unreacted pockets behind the detonation front and usually requires rather larger source energy.

PACS: 47.40.Rs, 47.85.Gj, 82.40.Fp DOI: 10.1088/0256-307X/34/5/054701

A detonation wave consists of a leading shock followed by a thin reaction zone and exhibits one-dimensional (1D) pulsation instability or multi-dimensional cellular instability. Lee *et al.*[1] and Bourlioux *et al.*[2] provided an overall review of linear analysis of detonation instability. Short *et al.*[3,4] studied the instability of steady planar detonation by nonlinear analysis. Ng *et al.*[5] have found that the intrinsic instability can suppress a successful initiation of 1D detonation. Eckett *et al.*[6] have also found that detonations in 1D cylindrical geometries form initially and are subsequently killed by pulsation instability for near-critical initiation energy. Specially, Watt *et al.*[7] investigated pulsation instability of weakly curved detonation and found that curvature was able to destabilize the detonation. Many previous simulations[8–12] have been conducted to study multi-dimensional detonations propagating in ducts. However, global curvature has a significant effect on their propagations.[13–17] Recently, researchers have been devoted to the study of cellular detonation with global curvature.[18–20] Redulescu *et al.*[18] conducted experiments in porous wall tubes to clarify the role of transverse waves in real detonation with weakly curved front. The numerical results obtained by Mahmoudi *et al.*[20] have shown that the increased front curvature leads to the difficulty in sustaining propagation for both regular and irregular detonations. Jackson *et al.*[21] and Lee *et al.*[22] have found that the Mach-shock curvature is an origin of detonation cell divergence. Jiang *et al.*[19] observed numerically diverging and self-organized front for cylindrical detonations. Jiang *et al.*[23] simulated the 2D propagation of cylindrical detonations and found cell bifurcation. However, the effect of cellular instability on the initiation of cylindrical detonations is still unclear. Consequently, the objective of this study is to reveal the effect of cellular instability on the initiation of stable and unstable detonations in 1D and two-dimensional (2D) cylindrical geometries.

The reactive flow Euler equations are used to describe detonation propagation, as seen in the previous study.[24] The heat of reaction per unit volume and the specific heat ratio are 50 and 1.2, respectively, in the present simulations. The reaction rate is given by the Arrhenius law $\omega = -KY\exp(-E_{\rm a}/R_{\rm u}T)$, where $E_{\rm a}$ is the activation energy, $R_{\rm u}$ is the molar gas constant, and K is the constant pre-exponential factor. All physical variables are made dimensionless based on the state of unreacted gas. For steady planar detonation, the C-J detonation velocity is given by

$$D_{\rm C-J} = \sqrt{(\gamma^2-1)Q/2} + \sqrt{(\gamma^2-1)Q/2 + \gamma p_0/\rho_0}.$$

For a curved front of radius R, the detonation speed is given by[25–27]

$$D = \sqrt{\gamma p_0[(p_{\rm s}/p_0 - 1)(\gamma-1)/2\gamma + 1]},$$

where $p_{\rm s}$ is the shock pressure.

To numerically solve the Euler equations, we apply the 5th-order local characteristic-based weighted essentially non-oscillation (WENO) conservative finite difference schemes[22,28–30] for the space discretization and the third-order TVD Runge–Kutta[31,32] for time discretization. To construct a WENO scheme, a set of substencils are used to adapt to a higher order polynomial approximation at smooth parts of the solution or to a lower order polynomial approximation that avoids interpolation across discontinuities, in which a nonlinear convex combination of lower order polynomials is required. A local rate of convergence is yielded when the convex combination of local lower order polynomials is applied at smooth parts of the solution. In addition, positivity-preserving high order WENO finite difference schemes are further constructed. A positivity-preserving limiter is added to the WENO finite difference scheme to preserve the positivity of

*Supported by the National Natural Science Foundation of China under Grant Nos 91541206 and 91441131.
**Corresponding author. Email: huangjingold@foxmail.com
© 2017 Chinese Physical Society and IOP Publishing Ltd

pressure and density, and to maintain the conservation of conserved variables and high-order accuracy of numerical solutions as the CFL condition is given suitably. Relative grid resolution is verified so that it can reach the fifth-order resolution.[24]

For the 1D case, the reflective boundary condition is set at $R = 0$, while the free outflow condition is at $R = \infty$, where R is the radius. For the 2D case, a square computational domain is filled with unreacted gas; symmetric boundary conditions are set respectively at the lines $x = 0$ and $y = 0$, while the other sides are the free outflow conditions. A source energy E_s is set at the origin to initiate a cylindrical detonation. Grid resolution of 20 points per half-reaction zone is used to mesh the computational domain. Due to the large number of cells in the 2D simulations, it is essential to implement the high-resolution and efficient parallel code on a massive parallel platform, as it is carried out in this work by 360 processors.

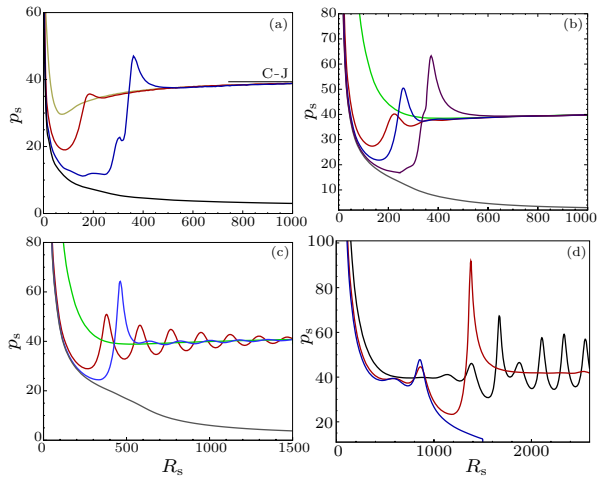

Fig. 1. Shock pressure p_s as a function of the shock radius R_s for 1D detonations with different source energies and activation energies: (a) $E_a = 15$ and $E_s = 1200$ (green line), 1000 (red line), 800 (blue line) and 700 (black line); (b) $E_a = 20$ and $E_s = 10000$ (green line), 6000 (red line), 5000 (blue line), 4100 (purple line) and 4000 (gray line); (c) $E_a = 24$ and $E_s = 30000$ (green line), 12000 (red line), 7000 (blue line) and 6000 (black line); and (d) $E_a = 27$ and $E_s = 90000$ (black line), 38000 (red line) and 30000 (blue line).

In general, $E_a \sim 24$ is the neutral stability boundary. When E_a is in the range of 24–27, the corresponding detonations usually are weakly unstable. Hence, we chosen $E_a = 15$, 20, 24 and 27 to conduct the present 1D and 2D simulations. Figure 1 shows the shock pressure p_s as a function of the shock radius R_s for 1D detonations with different activation energies. For $E_a = 15$, the source energy of $E_s = 700$ fails to achieve the initiation, with the shock pressure decreasing initially to $\sim$10 at $R_s \sim 200$ (here tilde denotes proximately equal) and eventually tending to be zero; see the black line in Fig. 1(a). For $E_s = 800$, the successful initiation can be triggered by the strong pressure pulse (abrupt pressure rise) appearing after the rapid decay of the initial blast waves, see the blue line in Fig. 1(a). Therefore, there exists a critical initiation energy between $E_s = 700$ and 800. For $E_s = 1200$, the pressure pulse does not appear. For $E_a = 20$, the shock pressure with $E_s = 10000$ decays smoothly to the C-J state; see the green line in Fig. 1(b). For $E_s = 6000$, the shock pressure behaves as weak oscillations in the range of radius with large curvature, see the red line in Fig. 1(b). For $E_s = 5000$ and 4100, the strong pressure pulses trigger the successful initiation. However, for $E_s = 4000$ the initiation fails. Hence, the critical initiation energy exists between $E_s = 4000$ and 4100 and is higher than that in the case of $E_a = 15$.

Figure 1(c) shows the initiation behaviors of detonations with $E_a = 24$. It is seen that for $E_s = 30000$ the shock pressure decreases smoothly to the steady solution. For $E_s = 12000$, the pulsation instability appears at the radius where the curvature is large, and the oscillating amplitude of the shock pressure damps with increasing the shock radius.[13,33,34] For $E_s = 7000$, the shock pressure drops to the minimum; subsequently it jumps to a peak value, and then decreases rapidly and tends to be the steady solution, indicating that the initiation is successful. For $E_s = 6000$, the detonation eventually quenches. Hence, the critical initiation energy exists between $E_s = 7000$ and 6000.

Figure 1(d) shows the initiation behaviors of detonations with different source energies for $E_a = 27$. It is seen that for $E_s = 90000$ the shock pressure exhibits the irregular pulsation at $R_s \sim 1000$–2000 and eventually develops into the regular pulsation, which agrees with that in Ref. [13]. For $E_s = 38000$, the shock pressure behaves as small oscillations at $R_s \sim 600$–900, and then decreases rapidly and drops to $\sim$20 at $R_s \sim 1200$; subsequently it jumps to a much higher value, and then decreases rapidly and tends to the steady solution, indicating that the initiation is achieved. For $E_s = 30000$, as the detonation decays to the C-J state, the shock pressure exhibits a weak oscillation at $R_s \sim 500$–700, indicating that the initiation has formed during this period; after undergoing a relatively strong pressure pulse at $R_s \sim 700$–900, it decreases rapidly and is below $\sim$15, indicating that the detonation quenches. This demonstrates that the pulsation instability can kill the detonation that has formed. It is also known that the critical initiation energy exists between $E_s = 30000$ and 38000. In a word, with increasing the activation energy the initiation of 1D cylindrical detonations is more difficult.

According to the 1D cases, we select suitable source energies to carry out the corresponding 2D simulations. For $E_a = 15$, the 1D initiation can be obtained through the subcritical initiation path for the detonation with $E_s = 1000$. Hence, $E_s = 1000$ is selected as the source energy to simulate 2D initiation. Figure 2 shows the front structures of cylindrical detonations with different activation energies. It is seen that at $R_s \sim 300$ the global detonation structure is thin and smooth, containing many triple points shown in Fig. 2(a). Simultaneously, the shock couples with the reaction layer and the gas entering the front is burnt out.

For $E_a = 20$, the source energy of $E_s = 6000$ are selected to simulate the corresponding detonations in the 2D cylindrical geometries since it is subcritical for

the 1D initiation. Typical front structures are shown in Fig. 2(b). It is seen that the global detonation structure is elongated and unreacted pockets enter slip layers behind the front. Some small-scale vortices in the surfaces of slip layers are observed due to the K-H instability, resembling the feature captured in the experiments of Redulescu *et al.*[18] and Mahmoudi *et al.*[20] The unreacted pockets lead to difficulty in the 2D initiation. Nevertheless, the detonation characterized by the lower activation energy can be initiated successfully by the source energy of $E_s = 6000$, by which the corresponding 1D initiation shown in Fig. 1(b) can also be achieved.

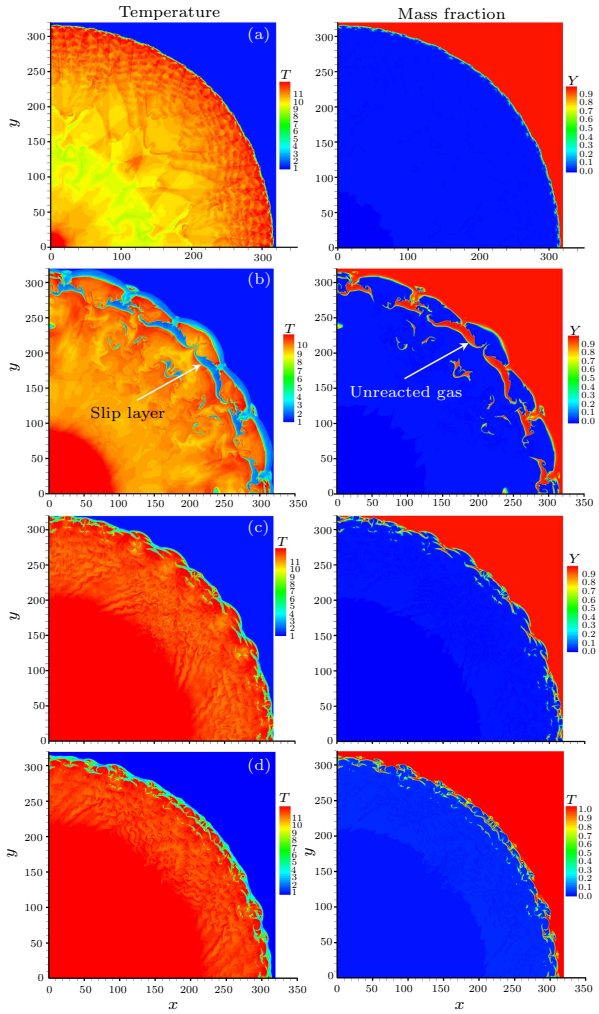

Fig. 2. Frontal structures of 2D cylindrical detonations: (a) $E_a = 15$ and $E_s = 1000$; (b) $E_a = 20$ and $E_s = 6000$; (c) $E_a = 24$ and $E_s = 30000$; and (d) $E_a = 27$ and $E_s = 90000$.

For $E_a = 24$, $E_s = 30000$ and 12000 are selected to carry out 2D simulations because they correspond respectively to the supercritical and subcritical paths for the 1D initiation. Figure 2(c) shows that for $E_s = 30000$, the unreacted pockets remain downstream as the detonation decays to the C-J state at $R_s \sim 300$; the 2D initiation can be achieved. For $E_s = 12000$, the 1D detonation can be initiated successfully, while the corresponding 2D initiation fails; see Fig. 3(a). Consequently, the 2D initiation must be achieved through a supercritical initiation way.

Note that from Fig. 2(d), for $E_a = 27$ the unreacted pockets have appeared at $R_s \sim 300$ even if the detonation still is overdriven. The unreacted pockets consequently make the 2D initiation more difficult. Furthermore, $E_s = 38000$ is able to initiate successfully the 1D simulation, while it is not enough to initiate the 2D detonation, see Fig. 3(b). This demonstrates that the negative effect of cellular instability on the initiation of the cylindrical detonation is enhanced as the activation energy increases.

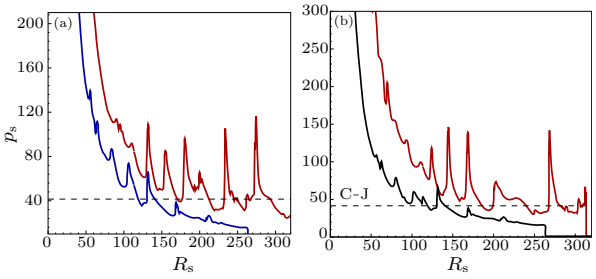

Fig. 3. Shock pressure p_s as a function of shock radius R_s for 2D detonations with different source energies: (a) $E_a = 24$ and $E_s = 30000$ (red line), 12000 (blue line); (b) $E_a = 27$ and $E_s = 90000$ (red line), 38000 (black line).

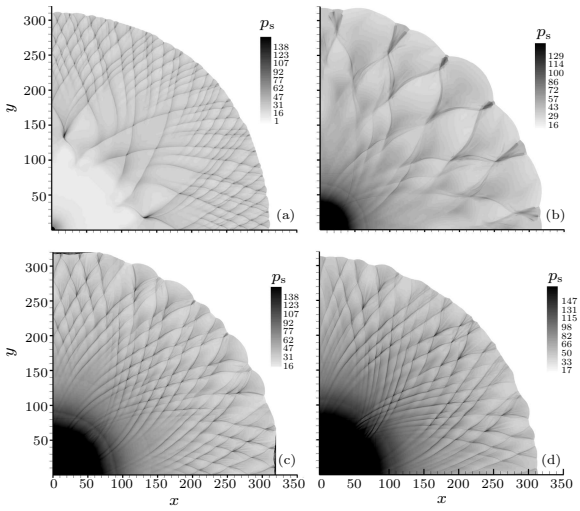

Fig. 4. Cell evolution of cylindrical detonation: (a) $E_a = 15$ and $E_s = 1000$; (b) $E_a = 20$ and $E_s = 6000$; (c) $E_a = 24$ and $E_s = 30000$; and (d) $E_a = 27$ and $E_s = 90000$.

Figure 4 shows the cell evolution of cylindrical detonations with different activation energies. For $E_a = 15$, the source energy of $E_s = 1000$ used in the 1D simulation can also initiate successfully the 2D cylindrical detonation; initially overdriven detonation decays rapidly at $R_s \sim 0$–120 and hence there is no cell. In this stage the downstream flow velocity increases and eventually reaches the sonic state, and thereby cuts off the downstream influence and then leads to re-intensification of the reaction rate. The leading shock is re-intensified and initiates the cellular detonation. The divergence of the cells is also observed at $R_s > 120$, see Fig. 4(a). For the cylindrical detonation with $E_a = 20$ and $E_s = 6000$, the cell is globally regular, with finer structures, as shown in Fig. 4(b). At $R_s \sim 180$, the detonation propagates at a speed below the C-J value and it can still sustain at $R_s \sim 300$,

substantiating that the initiation is successful. Hence, the 2D cylindrical detonation with $E_a = 20$ can be initiated through the subcritical initiation path. Figure 4(c) shows the cell evolution of the cylindrical detonation with $E_a = 24$ and $E_s = 30000$. It is seen that as the overdriven detonation decays, the cells form at $R_s \sim 150$ and then diverge at $R_s \sim 300$ to sustain the detonation. For $E_a = 27$ and $E_s = 90000$, the cells can be formed in the decay of more overdriven detonation and the finer cell structures are observed in Fig. 4(d), as compared with the 2D case for $E_a = 24$. Hence, it is confirmed further that for $E_a = 24$ and 27 the 2D initiation usually requires larger source energy and is obtained through the supercritical initiation path.

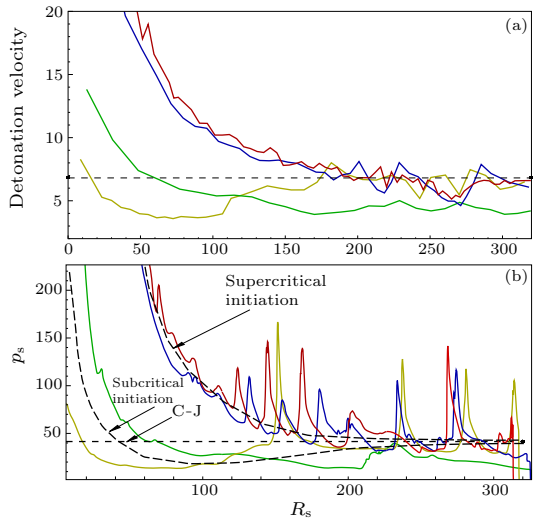

Fig. 5. Average detonation velocity and shock pressure versus shock radius for 2D detonations: $E_a = 15$ and $E_s = 1000$ (coppery line); $E_a = 20$ and $E_s = 10000$ (green line); $E_a = 24$ and $E_s = 30000$ (blue line); $E_a = 27$, $E_s = 90000$ (red line).

Figure 5 shows the change of average velocity and shock pressure with shock radius for 2D detonations. It is seen that the 2D initiation can be achieved through a subcritical initiation way for $E_a = 15$ and 20, while it becomes more difficult for $E_a = 24$ and 27. Hence, the negative effect of cellular instability on the 2D initiation is amplified by increasing the activation energy because burning of the unreacted pockets is more related to the diffusion that is absent in the present Euler simulation.

From the above discussions, it is known that the 2D initiation of cylindrical detonations is more difficult than that predicted in the 1D case due to cellular instability. For the lower activation energy, the source energy used in the 1D is able to produce the cellular detonation. For the higher activation energy, cellular instability results in increasing difficulty in the 2D initiation, which is also largely amplified by the reduction of source energy. Consequently, larger source energy is required to achieve the sustaining cylindrical detonation. Otherwise, the detonation is prone to becoming quenched during the decay.

In summary, cellular instability suppresses significantly the initiation of 2D detonations in cylindrical geometries, and the successful 2D initiation requires higher source energy than that in 1D simulations. For the lower activation energy, the 2D initiation is obtained by the subcritical initiation path. However, for the high activation energy, the difficulty in the 2D initiation increases due to unreacted pockets caused by cellular instability. Consequently, the detonation is prone to becoming quenched by reducing source energy.

The above conclusions are drawn in the context of weakly unstable detonations without viscosity.[35] In fact, the cellular structure on the front also has a positive effect on the initiation process observed in some other studies,[36,37] in which the initiation is related to the frequency of the perturbation imposed under the initial condition. This reverse tendency is also observed for the case with $E_a > 30$, in which the cellular instability is easier to be amplified because significant flow instability and viscosity may play significant roles on the initiation. This problem merits further study.

References

[1] Lee H I and Stewart D S 1990 *J. Fluid Mech.* **216** 103
[2] Bourlioux A and Majda A J 1992 *Combus. Flame* **90** 211
[3] Short M and Stewart D S 1998 *J. Fluid Mech.* **368** 229
[4] Short M 2001 *J. Fluid Mech.* **430** 381
[5] Ng H D and Lee J H S 2003 *J. Fluid Mech.* **476** 179
[6] Eckett C A et al 2000 *J. Fluid Mech.* **421** 147
[7] Watt S D and Sharpe G J 2004 *Proc. R. Soc. London Ser. A* **460** 2551
[8] Sharpe G J and Falle S A E G 2000 *Combust. Theor. Model.* **4** 557
[9] Deledicque V and Papalexandris M V 2006 *Combust. Flame* **144** 821
[10] Shen H et al 2011 *Chin. Phys. Lett.* **28** 124705
[11] Huang Y et al 2012 *Chin. Phys. Lett.* **29** 114701
[12] Liu S J et al 2011 *Chin. Phys. Lett.* **28** 094704
[13] Watt S D and Sharpe G J 2005 *J. Fluid Mech.* **522** 329
[14] Wang C et al 2008 *Appl. Math. Mech.* **29** 1487
[15] Dong G and Fan B C 2011 *Chin. J. High Press. Phys.* **25** 193
[16] Han G L, Jiang Z L, Wang C and Zhang F 2008 *Chin. Phys. Lett.* **25** 2125
[17] Wang G et al 2010 *Chin. Phys. Lett.* **27** 024701
[18] Redulescu M I and Lee J H S 2002 *Combust. Flame* **131** 29
[19] Jiang Z L et al 2009 *Combust. Flame.* **156** 1653
[20] Mahmoudi Y and Mazaheri K 2015 *Acta Astronaut.* **115** 40
[21] Jackson S I and Short M 2013 *Combust. Flame* **160** 2260
[22] Lee J H et al 1972 *Combust. Flame.* **18** 321
[23] Jiang Z L et al 2008 *Chin. Phys. Lett.* **25** 3704
[24] Han W et al 2015 *Phys. Fluids* **27** 106101
[25] Yao J and Stewart D S 1996 *J. Fluid Mech.* **309** 225
[26] He L 1996 *Combust. Flame* **104** 401
[27] Chung K L 2006 *Combustion Physics* (Cambridge: Cambridge University Press)
[28] Jiang G S and Shu C W 1996 *J. Comput. Phys.* **126** 202
[29] Shu C W and Osher S 1988 *J. Comput. Phys.* **77** 439
[30] Balsara D S and Shu C W 2000 *J. Comput. Phys.* **160** 405
[31] Wang C et al 2013 *Combust. Flame* **160** 447
[32] Zhang X and Shu C W 2012 *J. Comput. Phys.* **231** 2245
[33] He L and Clavin P 1994 *J. Fluid Mech.* **277** 227
[34] Sharpe G J and Falle S A E G 2000 *J. Fluid Mech.* **414** 339
[35] Radulescu M I et al 2007 *21th The International Colloquium on the Dynamics of Explosions and Reactive Systems* (Poitiers France 23–27 July 2007)
[36] Ng H D et al 2015 *25th The International Colloquium on the Dynamics of Explosions and Reactive Systems* (Leeds UK 2–7 August 2015)
[37] Ng H D et al 2001 *18th The International Colloquium on the Dynamics of Explosions and Reactive Systems* (Washington DC 29–31 July 2001)